Complexity Project: Understanding self-organised criticality in the Oslo model

I Kit Cheng
CID: 00941460

18th February, 2019

Abstract: Self-orgainsed criticality behaviour was demonstrated using simulations of the 1-dimensional Oslo rice pile model. Systems of size $L = [4, 8, 16, 32, 64, 128, 256, 512]$ were all driven with $N = 10^6$ grains. First, the average height and cross-over time of the piles were calculated to validate the algorithm. Using theoretical arguments, data-collapse was performed on the height of each pile, height probability $P(h; L)$ and avalanche-size probability $P(s; L)$. Finally, the scaling behaviour of cross-over time $t_c(L)$, pile height $h(L)$, standard deviation of height $\sigma_h(L)$ and slope $\sigma_{\langle z \rangle}(L)$, and k^{th} moments $\langle s^k \rangle(L)$ with system size were obtained, taking into consideration corrections to finite-size scaling.

Word count: 2481

1 Introduction

The Oslo model is one of the simplest models displaying self-organised criticalty. This behaviour is characterised by the system's ability to reach a recurrent steady-state without the need to fine-tune external parameters and by its scale-free behaviour which means its properties follow a power law distribution in the asymptotic limit [1]. For example, a rice pile will form as grains are slowly added repeatedly. The size of the pile is only limited by the size of the surface on which it rests. Eventually, the pile will stop getting bigger and will have reached a recurrent state where the number of grains added equals the number of grains that leave the system through toppling. This is self-organisation. The number of topples (or avalanche size) will display a power-law distribution meaning that there are many small avalanches but once in a while an enormous avalanche occurs. This is criticality.

2 Task 1- The algorithm

2.1 Implementation of Oslo model

The 1-dimensional Oslo model is characterised by the system size L, representing the number of discrete sites (labelled $i = 1, 2, ..., L$) where grains can occupy, and the slope of each site $z_i = h_i - h_{i+1}$, where h_i is the number of grains at site i. The dynamics was implemented in four steps. First, an empty system of size L is initialised. A threshold slope $z_i^{th} \in \{1, 2\}$ is chosen for each site by comparing a random number between 0 and 1 with p, the probability of $z_i^{th} = 1$. Second, the system is driven by adding one grain to the leftmost site $i = 1$. The number of grains added represents the time t elapsed. Third, if the slope of a site exceeded the threshold slope, $z_i > z_i^{th}$, then site i relaxed by losing a grain, followed by choosing a new threshold slope for the relaxed site only. Fourth, the process is repeated from step two.

2.2 Devising and performing tests to validate the algorithm

Three measures were used to validate the code. The average height of the pile $\langle h(L) \rangle$ (defined as the average height of site $i = 1$), the average avalanche size $\langle s(L) \rangle$ and the cross-over time $t_c(L)$ (defined as the number of grains in the system before another addition induces a grain to leave the system for the first time). The time $t = t_c$ is the length of the transient period where the pile is building up to the crititcal point. Thus, averages were found by only considering times $t > t_c(L)$ when the system is in steady state.

For system sizes of $L = 16$ and $L = 32$ with $p = 0.5$, $\langle h(L) \rangle$ was measured to be 26.5 and 53.9 respectively which were consistent with known values [2]. $\langle s(L) \rangle$ was measured to be 16 and 32 respectively as expected because in steady state grains would on average topple L times to leave the system. For system size $L = 16$ with $p = 0$ and $p = 1$, the Oslo model is simplified to the 1-dimensional BTW model with unique double and single step staircase recurrent state respectively. Steady-state is reached when a right-angle triangle is formed with number of grains corresponding to $L(L+1)z^{th}/2$. This agrees with the observed $t_c = 272$ and $t_c = 136$ respectively. The BTW model is also characterised by constant avalanches of size L in steady state which is observed in the simulation.

The following measurements are done for system sizes $L = \{4, 8, 16, 32, 64, 128, 256, 512\}$, all driven with $N = 10^6$ grains at boundary site $i = 1$, with $p = 0.5$ as the probability for setting the threshold slope $z_i^{th} = \{1, 2\}$.

3 Task 2: The height of the pile $h(t; L)$

3.1 Task 2a: Height $h(t; L)$ vs time t

In this task, the height of the pile $h(t; L)$ was defined as the number of grains at site $i = 1$ as it is the highest point in the pile, and t represents the number of grains added. After each grain, the height value is stored in an array. The results $h(t; L)$ is plotted against t in a log-log plot (Figure 1).

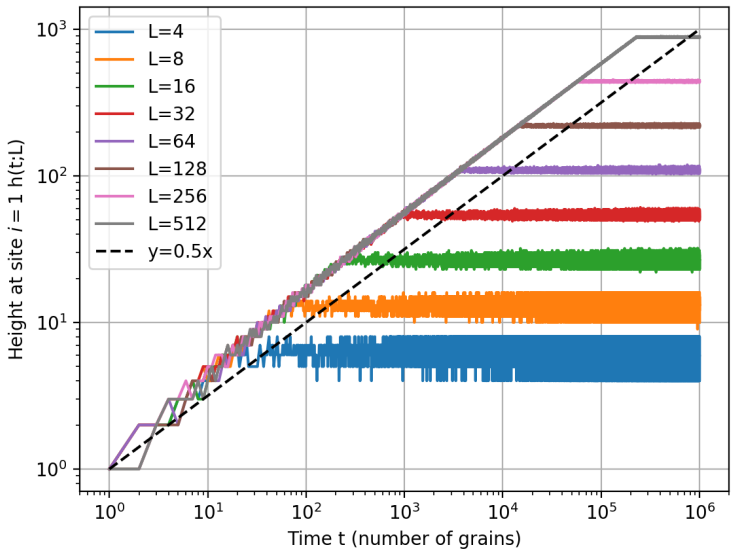

Figure 1: A log-log plot of $h(t; L)$ vs t for various system sizes L. There are two distinct regions. A linearly rising part corresponding to transient configurations and a flat part corresponding to recurrent configurations. A square-root relationship is plotted (dashed) for comparison.

This logarithmic plot reveals two distinct regimes that the piles encounter whilst being driven. Firstly, a region where $log(h)$ increased linearly with $log(t)$ with a slope of ≈ 0.5 indicating square root behaviour. Secondly, a region where $log(h)$ fluctuated around a constant value. These two regions correspond to the system being in a transient and recurrent configuration respectively. A configuration is a snapshot of the pile where the height at each site is specified. So, a transient configuration is one that only occurs once (i.e. never get the same snapshot again), since no grains are lost from the system during the transient period. The identical slopes for all system sizes implies that all piles fill up in the same way. Eventually, the height saturates due to a finite size system. Now, the system is in a recurrent configuration which can occur more than once, since grains can start falling out of the system allowing configurations to be re-visited. The steady state height of a pile increases with system size as expected.

3.2 Task 2b: Theoretical scaling behaviour of height $\langle h \rangle$ and cross-over time $\langle t_c \rangle$ with system size L

The scaling of height and cross-over time with system size can be derived by considering the pile as a right-angle triangle in the steady state. For $L \gg 1$, the pile slope can be assumed constant on average (edge effects negligible). Using the definition that slope is height divided

by base, the average height is expected to scale linearly with system size as

$$\langle h \rangle = \langle z \rangle L. \tag{1}$$

The cross-over time is analogous to the number of grains in the system which is equivalent to the area under the triangle. The area scales as height x base proportional to L x L. Thus, the cross-over time is expected to scale as

$$t_c \propto L^2. \tag{2}$$

3.3 Task 2c: Data collapse for averaged height $\tilde{h}(t; L)$ vs time t

For this task, the height data is smoothed by simulating each system size M times to calculate an average height $\tilde{h}$:

$$\tilde{h}(t; L) = \frac{1}{M} \sum_{i=1}^{M} h_i(t; L) \tag{3}$$

where $h_i(t; L)$ is the height at time t in the i^{th} simulation of system size L.
$L = \{4, 8, 16, 32, 64, 128, 256, 512\}$ were simulated $M = \{60, 30, 20, 10, 10, 10, 10, 5\}$ times respectively for the smoothing (see Figure 2a for results).

Using the fact that $\langle h \rangle \propto L$ and $\langle t_c \rangle \propto L^2$ from task 2b, the height was re-scaled with L and time with L^2, resulting in a data collapse for $\tilde{h}(t; L)/L$ against t/L^2 (Figure 2b). This removes the L dependence for all the systems to reveal the underlying scaling behaviour. Mathematically, the scaling function $\mathcal{F}$ relates the collapsed variables through $\tilde{h}(t; L) = L\mathcal{F}(t/L^2)$. For small time $t \ll L^2$, the effect of a finite size system is not felt as the grains have not reached the edge yet. This means $\tilde{h}(t; L)$ should have no L dependence implying that $\tilde{h}(t; L) = LC_1\sqrt{t/L^2} = \sqrt{t}$ (independent of L). Thus, $\mathcal{F}(x) = C_1\sqrt{x}$. Indeed, a linear regression on the transient part of $L = 512$ (dashed line in Figure 2b) gives a slope of 0.51 and constant $C_1 = exp(0.62) = 1.86$. Examining Figure 2b more closely, the transient tail deviates more from $\mathcal{F}$ for smaller systems because of corrections to scaling. For large time $t \gg L^2$, the height is proportional to L (as argued in Task 2b). Thus, $\mathcal{F}(x) = C_2 = 1.73$, found by averaging over the heights in the recurrent regime.

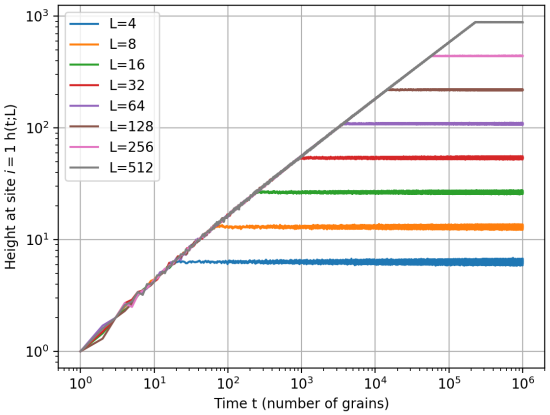

(a) Smoothed height vs time.

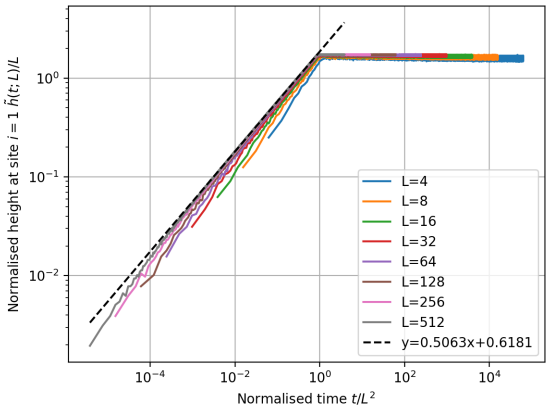

(b) Data collapse of smoothed height vs time.

Figure 2: (a) The smoothing reduced fluctuations in both the transient and recurrent part. (b) The data collapse scaled all $t_c = 1$ and all recurrent heights to a constant just under 2.

3.4 Task 2d: Scaling of cross-over time $\langle t_c \rangle$ with system size L

The definition of cross-over time is

$$t_c(L) = \sum_{i=1}^{L} z_i.i \tag{4}$$

where z_i are the local slopes in the system to which an added grain induces a flow out of the system for the first time. By assuming that $\langle z_i \rangle = \langle z \rangle$ (which is reasonable for $L \gg 1$ as edge effects become negligible), the average cross over time can be calculated by averaging $t_c(L)$ over M simulations of the same system size L. Mathematically,

$$\begin{aligned}
\langle t_c(L) \rangle &= \frac{1}{M} \sum_{m=1}^{M} \left(\sum_{i=1}^{L} z_{i,m}.i \right) = \sum_{i=1}^{L} i \left(\sum_{m=1}^{M} \frac{z_{i,m}}{M} \right) && \text{Addition is commutative} \\
&= \sum_{i=1}^{L} i \langle z_i \rangle && \text{By definition of } \langle z_i \rangle \\
&= \langle z \rangle \sum_{i=1}^{L} i && \text{Assuming } \langle z_i \rangle = \langle z \rangle
\end{aligned}$$

Thus, the theoretical expression for $\langle t_c(L) \rangle$ is

$$\langle t_c(L) \rangle = \frac{\langle z \rangle}{2} L^2 \left(1 + \frac{1}{L} \right). \tag{5}$$

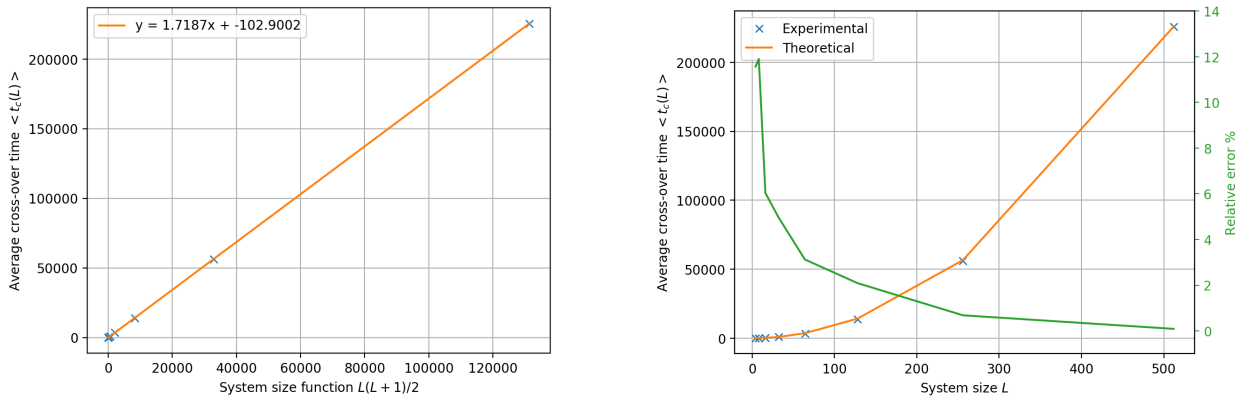

(a) (b)

Figure 3: (a) A plot of t_c vs. $L(L+1)/2$ to extract the average slope $\langle z \rangle$. (b) A plot of $\langle t_c(L) \rangle$ vs L comparing theory and simulation data. The green line shows the relative error.

This expression shows the average cross-over time correction to scaling term $(1/L)$ which becomes negligible for large L, agreeing with $t_c \propto L^2$ derived in task 2b. To find $\langle z \rangle$, the measured $\langle t_c(L) \rangle$ is plotted against $(L + \frac{1}{L})/2$ revealing a straight line (see Figure 3a) as expected from theory. The slope gives an estimate of $\langle z \rangle \approx 1.72$. In Figure 3b, the simulation values of $\langle t_c(L) \rangle$ is plotted against the corresponding L. Using the above equation with $\langle z \rangle = 1.72$, the theoretical values of $\langle t_c(L) \rangle$ are overlaid onto the same plot. At first, it seems like a perfect fit to data. However, the relative error $|t_{c,theory} - t_{c,expt}|/t_{c,expt})$ shows a substantial error greater than 10% for $L < 16$. This is expected as the assumption that $\langle z_i \rangle = \langle z \rangle$ is not very good for small L when edge effects are significant.

3.5 Task 2e: Scaling of averaged height $\langle h \rangle$ with system size L

The average height as argued in task 2b scales as $\langle h \rangle \propto L$. So, $\langle h \rangle / L = constant$ should be independent of L. If this were true, the plot of $\langle h \rangle / L$ against L should produce a flat line. However, a curved line is seen in Figure 4a, revealing the corrections to scaling for small L. This can be explained by assuming the following form of the corrections to scaling $\langle h(t;L) \rangle = a_0 L(1 - a_1 L^{-\omega_1} + a_2 L^{-\omega_2} +)$ where $\omega_i > 0$ and a_i are constants. Neglecting terms with $i > 1$ means

$$\langle h(t;L) \rangle = a_0 L(1 - a_1 L^{-\omega_1}). \tag{6}$$

Taking the log of both sides gives $log(\frac{\langle h \rangle}{L}) = log(a_0) + log(1 + a_1 L^{-\omega_1})$, where the second term accounts for the deviation from the constant seen in Figure 4a. This equation implies that as $L \to \infty$, then $a_0 \to \frac{\langle h \rangle}{L}$. In other words, a_0 is the average slope for an infinite system. Therefore, it is not possible to get the true a_0 from a finite system of size L. To estimate the parameters a_0 and ω_0, equation 6 is rearranged to get

$$a_0 - \frac{\langle h \rangle}{L} = a_0 a_1 L^{-\omega_1}. \tag{7}$$

Taking the log of both sides gives $log(a_0 - \frac{\langle h \rangle}{L}) = -\omega_1 log(L) + log(a_0 a_1)$. This equation is of the form $y = mx + c$. Hence, plotting $(a_0 - \langle h \rangle / L)$ vs L in log-log scale reveals a straight line after fine-tuning the parameter a_0 (see Figure 4b). This is done quantitatively by maximising the Pearsons coefficient giving $a_0 = 1.738$. The slope thus gives an estimate of the parameter $\omega_1 = 0.532$.

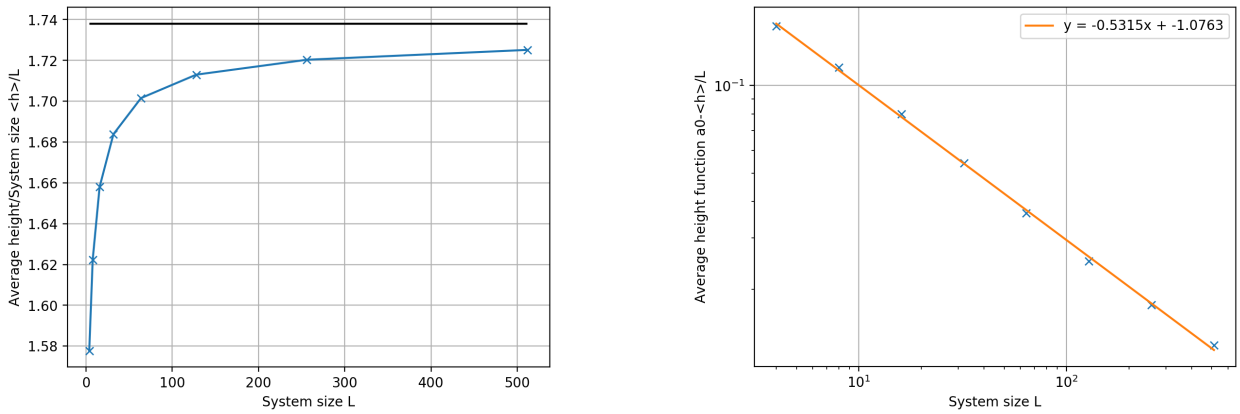

(a) (b)

Figure 4: (a) A plot of $\langle h \rangle / L$ vs. L revealing significant corrections to scaling for small L. (b) A plot of $a_0 - \frac{\langle h \rangle}{L}$ vs L for extracting the parameters a_0 and ω_1 used in the corrections to scaling for $\langle h \rangle$.

3.6 Task 2f: Scaling of standard deviation of height σ_h and of slope σ_z with system size L

The standard deviation of the height represents the how much the height fluctuates from its constant steady state value. It is defined as

$$\sigma_h(L) = \sqrt{\frac{1}{N-t_c}\sum_{t=t_c+1}^{N} h^2(t;L) - \left(\frac{1}{N-t_c}\sum_{t=t_c+1}^{N} h(t;L)\right)^2}, \tag{8}$$

where t_c is the cross-over time and $t > t_c$ is in the recurrent regime. To reveal how σ_h scales with system size, a plot of σ_h vs L in a log-log plot shown in Figure 5a reveals a power-law relationship

$$\sigma_h(L) \propto L^{0.24} \tag{9}$$

where the exponent value is obtained from the slope. This implies that as $L \to \infty$, $\sigma_h \to \infty$ too. The average slope is $\langle z \rangle = \frac{\langle h \rangle}{L}$, which means the standard deviation of slope is

$$\sigma_z(L) = \frac{\sigma_h}{L} \propto L^{-0.76}, \tag{10}$$

using the above result for σ_h. This implies that in the limit $L \to \infty, \sigma_z(L) \to 0$ and $\langle z \rangle \to a_0$ (a delta function centred at a_0), as mentioned in task 2e. Indeed, a plot of $\sigma_z(L)$ vs L shown in Figure 5b reveals an exponent of approximately -0.76, as expected. Note that the linear regression line for both plots only included points with $L > 32$ to minimise error from corrections to scaling.

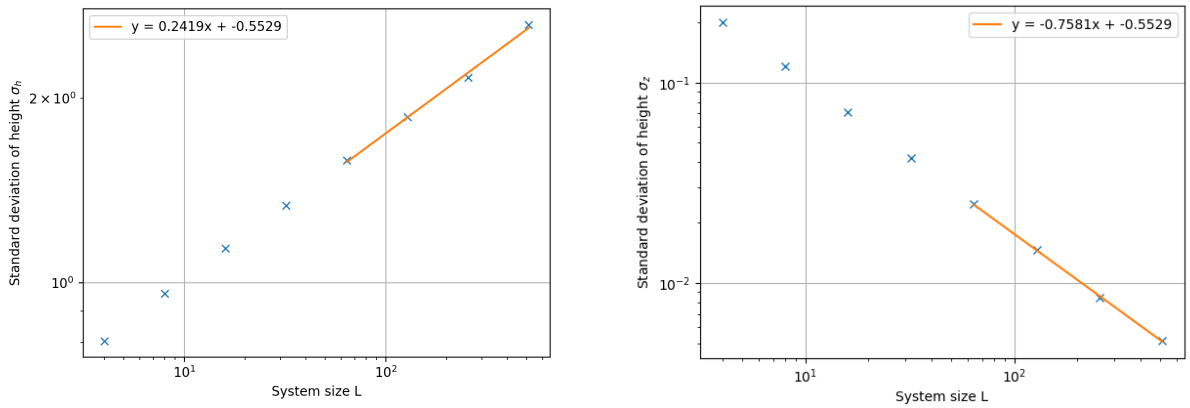

(a) (b)

Figure 5: (a) A plot of $\sigma_h(L)$ vs. L revealing a power-law relationship with exponent 0.24. (b) A plot of $\sigma_z(L)$ vs L revealing a power-law decay relationship with exponent -0.76.

3.7 Task 2g: Data collapse for height probability $P(h;L)$ vs h

The height probability $P(h;L)$ gives the probability that the pile has a particular height in the recurrent regime. Assuming that local slopes z_i are independent, with the same distribution and finite variance, the height $h = \sum_{i=1}^{L} z_i$ for $L \gg 1$, is expected to take the form of a Gaussian distribution via the central-limit theorem; which states that the sum of

many independent random variables tends toward a Gaussian. The height probability would also be Gaussian since it is just normalised,

$$P(h;L) = \frac{1}{\sigma_h\sqrt{2\pi}} e^{\frac{-(h-\langle h\rangle)^2}{2\sigma_h^2}}. \tag{11}$$

The experimental value of $P(h;L)$ was found by counting the number of each height and normalising with the total number of heights in the recurrent regime. A plot of the experimental $P(h;L)$ vs h for different system sizes is shown in Figure 6a. The curves all take the expected Gaussian form. The average height roughly increases linearly with L (i.e. $\langle h\rangle$ doubles if L doubles) and the standard deviation (width of the distribution) also increases with L, but sub-linearly.

By re-scaling the probability $P(h;L) \to \sigma_h P(h;L)$ and height $h \to (h - \langle h\rangle)/\sigma_h$, a data collapse for the various system sizes of P(h; L) can be produced. They should have the following form of a normalised Gaussian

$$P(h;L) = \frac{1}{\sqrt{2\pi}} e^{\frac{-h^2}{2}}. \tag{12}$$

A plot of $\sigma_h P(h;L)$ vs $(h - \langle h\rangle)/\sigma_h$ is shown in Figure 5b, overlaid is a Gaussian of mean 0 and standard deviation 1 as predicted from equation 12 . In general, the data traced out the Gaussian quite well. However, data points near the turning points of the Gaussian do not match theory exactly. This deviation is likely due to applying the central-limit theorem on a finite system (L not large enough). Furthermore, the assumption that z_i is independent is probably not true either since a site is more likely to topple if its neighbour had just toppled and thus the slopes are dependent on each other.

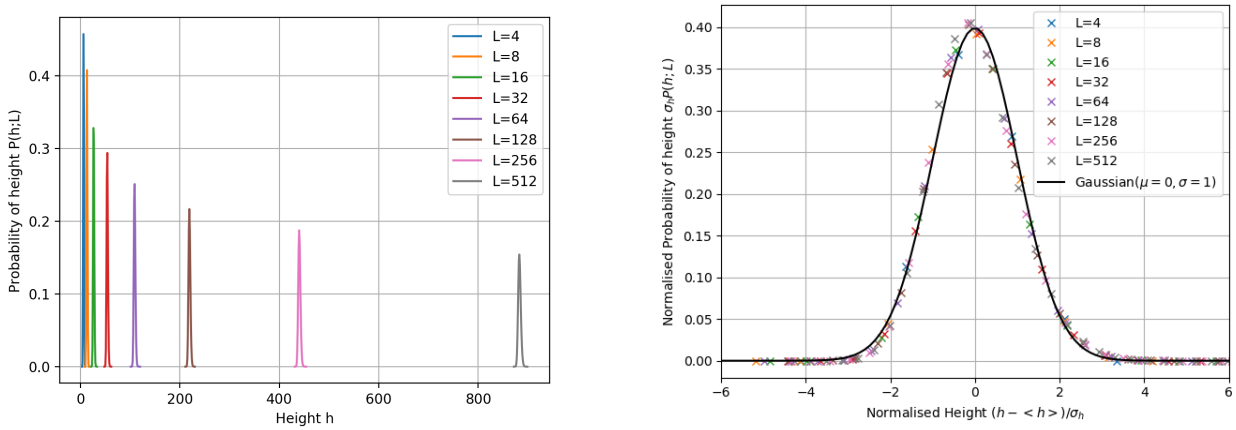

(a) (b)

Figure 6: (a) A plot of $P(h;L)$ vs h for various system sizes revealing the Gaussian nature of the distributions. The mean height increases linearly with system size and standard deviation (width) increases sub-linearly with system size.(b) A data collapse plot of $P(h;L)$ vs h for various system sizes compared with a Gaussian of mean 0 and standard deviation 1. The height probabilities of all system sizes approximately collapsed onto the same Gaussian.

4 Task 3: The avalanche-size probability $P(s; L)$

4.1 Task 3a: Binned avalanche-size probability $\tilde{P}(s; L)$ vs avalanche-size s

The avalanche size probability $P(s; L)$ gives the distribution of the avalanche sizes in the recurrent regime. It is calculated for $t > t_c$ as

$$P(s; L) = \frac{\text{No. of avalanches of size s in system of size L}}{\text{Total no. of avalanches}}. \tag{13}$$

The total number of avalanches is taken as $N - t_c(L)$ where $N = 10^6$ is the total number of grains added to each system. Its value is of order 10^5 for each system size. Figure 7 shows a log-log plot of the raw data and binned data for $P(s; L)$ vs s. As seen in the plot, the raw data contains rows of points for large s as these events only occurred once (so have the same $P(s; L)$). Thus, the data is binned using a logbin function with a scale parameter of 1.26 to extract the underlying distribution of $P(s; L)$. The scaling parameter determines the bin size. Starting from 1.0 meaning a bin size of 1, the value is incremented in steps of 0.1 until the binned data looked smooth.

The binned avalanche size probabilities show a power-law decay initially of the form $\tilde{P}(s; L) \propto s^{-\tau_s}$ with $\tau_s > 0$. This tells us that larger avalanches are less likely to occur. These scaling regions were identical for all system sizes which is evidence for the scale-invariance behaviour of the model. There is a bump at the end of the straight line which disrupts the power-law relationship, after which the avalanche size probability decays rapidly. Therefore, the avalanche size where the bump occurs can be thought of as the cut-off avalanche size s_c since bigger avalanches are extremely unlikely. The bumps are characteristics of a finite system since grains that make it to the edge will drop out, and hence restricts the maximum avalanche size allowed. Therefore, there is a preference for these avalanche sizes producing the excess probability bump. This cut-off avalanche size occurs at higher s as system size increases. For very small systems $L < 8$, the power-law scaling regime is very short.

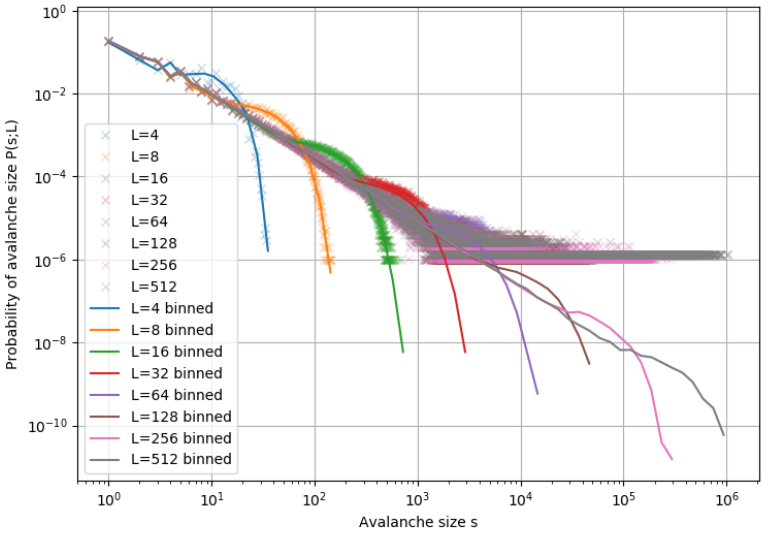

Figure 7: A plot of raw (crosses) and binned (line) data of $P(s; L)$ vs s for various system sizes. All system sizes displays the same underlying power-law decay until their respective bumps after which the probability decayed rapidly.

4.2 Task 3b: Data collapse for $\tilde{P}(s;L)$

The binned $\tilde{P}(s;L)$ was assumed to have the following finite-size scaling ansatz

$$\tilde{P}(s;L) \propto s^{-\tau_s}\mathcal{G}\left(\frac{s}{L^D}\right) \qquad \text{for } L \gg 1, s \gg 1 \ , \tag{14}$$

where D is the avalanche dimension, τ_s is the avalanche-size exponent, and $\mathcal{G}(x)$ is the finite-size scaling function. Rearranging this equation to $s^{\tau_s}\tilde{P}(s;L) \propto \mathcal{G}(s/L^D)$, a data collapse can be performed by plotting $s^{\tau_s}\tilde{P}(s;L)$ vs s/L^D on a log-log scale (Figure 8a); revealing the underlying finite-size scaling function which is approximately constant for small s and rapidly decays beyond the bump $s > s_c \gg 1$. τ_s is estimated from fitting a linear regression line to the power-law region $10 < s < s_c$ for $L = 512$, giving a value for $\tau_s \approx 1.556$ (Figure 8b). A large L is used for this to minimise corrections to scaling. This can also be achieved by fine-tuning τ_s until the bumps for $L > 32$ in the collapsed plot align to the same y-value, giving a similar value. Similarly, D is extracted by aligning the bumps for $L > 32$ in the collapsed plot to the same x-value, giving $D = 2.25$. These values agree reasonably well with the theoretical values for a boundary driven model which satisfies $D(2 - \tau_s) = 1$ (see Task 3c). Lines from smaller L do not fall onto the limiting scaling function $\mathcal{G}$ due to corrections to scaling. L^D can be interpreted as the cut-off avalanche size s_c, since a typical avalanche is associated with the system size L and the fluctuations in height $\sigma_h \propto L^{0.24}$. The maximum distance a grain can move is L. Hence, the cut-off (maximum) avalanche size $s_c \propto L^{0.24}LL = L^{2.24} \approx L^D$.

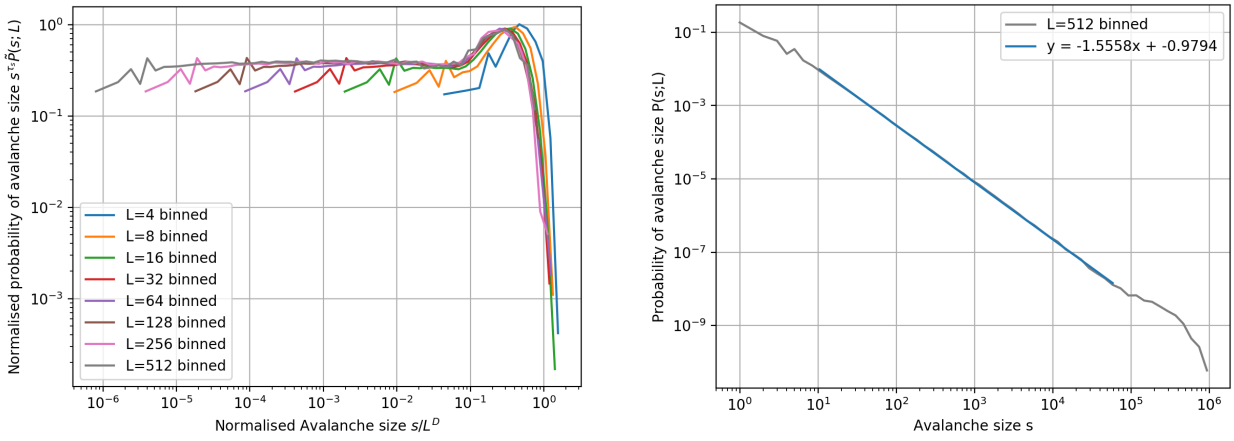

(a) (b)

Figure 8: (a) A data collapse plot of $s^{\tau_s}\tilde{P}(s;L)$ vs s/L^D for various system sizes revealing the underlying finite-size scaling function. The scaling function is constant for small avalanche sizes s and decayed rapidly for large s. (b) A plot of $P(s;L)$ vs s for $L = 512$ showing the regression line used to estimate the avalanche-size exponent τ_s.

4.3 Task 3c: Scaling of k^{th} moment $\langle s^k \rangle$ with system size L and moment analysis

Using moment analysis, the scaling of the k^{th} avalanche size moments $\langle s^k \rangle$ is determined. From the ansatz for $P(s; L)$ in task 3b, the k^{th} moment is

$$\begin{aligned}
\langle s^k \rangle &= \sum_{s=1}^{\infty} s^k P(s; L) \\
&= \sum_{s=1}^{\infty} s^{k-\tau_s} \mathcal{G}(\frac{s}{L^D}) \\
&\propto \int_1^{\infty} s^{k-\tau_s} \mathcal{G}(\frac{s}{L^D}) ds \\
&= \int_{1/L^D}^{\infty} (uL^D)^{k-\tau_s} \mathcal{G}(u) L^D du \\
&= L^{D(1+k-\tau_s)} \int_{1/L^D}^{\infty} u^{k-\tau_s} \mathcal{G}(u) du.
\end{aligned} \tag{15}$$

In the intermediate step, the sum can be approximated by an integral because the main contribution to $\langle s^k \rangle$ comes from $s \gg 1$ and thus the discrete nature of s become negligible. A substitution for $u = s/L^D$ is made as well. The integral term is finite because the scaling function decays rapidly for large s which ensures convergence in the infinite upper limit. Thus, $\langle s^k \rangle \propto L^{D(1+k-\tau_s)}$, for $L \gg 1, k \geq 1$. For $k = 1$, $\langle s \rangle \propto L$ is expected. This implies an exponent of 1 leading to an equation for the parameters

$$D(2 - \tau_s) = 1. \tag{16}$$

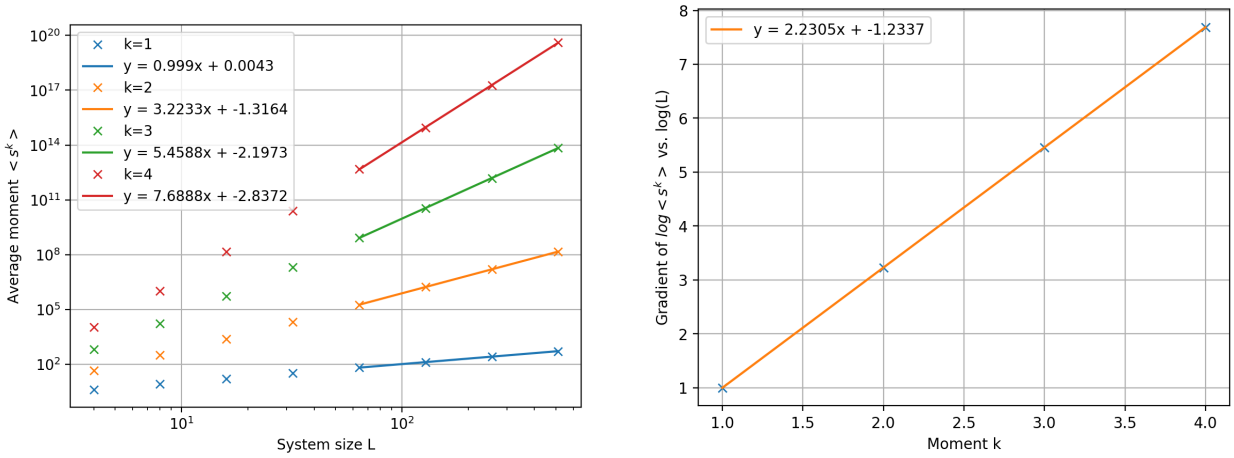

(a) (b)

Figure 9: (a) A plot of $\langle s^k \rangle$ vs L for various moments. The slope corresponds to the exponent in equation 15. (b) A plot of the moments slope in (a) vs k to reveal the avalanche dimension parameter D.

A plot of $\langle s^k \rangle$ vs L in log-log scale allows extraction of the exponent $D(1 + k - \tau_s)$ for different $k = \{1, 2, 3, 4\}$ (see Figure 9a) using the slope of a regression line. Only systems

with $L > 32$ are used to minimise corrections to scaling. Then, the slope values for each k are plotted against k, revealing a straight line (Figure 9b). This implies that $D(1+k-\tau_s) = mk+c$ where the slope $m = D$ and the intercept $c = D(1-\tau_s)$. Thus, the scaling parameters are calculated: $\tau_s = 1.55, D = 2.23$, with a precision of roughly 0.1 for both. These values derived from moment analysis agree quite closely to those found from fine-tuning graphically in task 3b, which means the ansatz is correct.

The assumption that $\langle s^k \rangle \propto L^{D(1+k-\tau_s)}$ implies that $\langle s^k \rangle L^{-D(1+k-\tau_s)} = constant$ should be independent of L. If this were true, the plot of $\langle s^k \rangle L^{-D(1+k-\tau_s)}$ against L should produce a flat line. However, Figure 10 shows that only $k = 1$ has this behaviour, whilst higher moments showed a curved line revealing the corrections to scaling for small L. Interestingly, the line curves up a bit at $L = 512$. To understand this behaviour, more data is needed from bigger system sizes. Nonetheless, the integral term in equation 15 cannot be considered as simply a constant as evident in Figure 10.

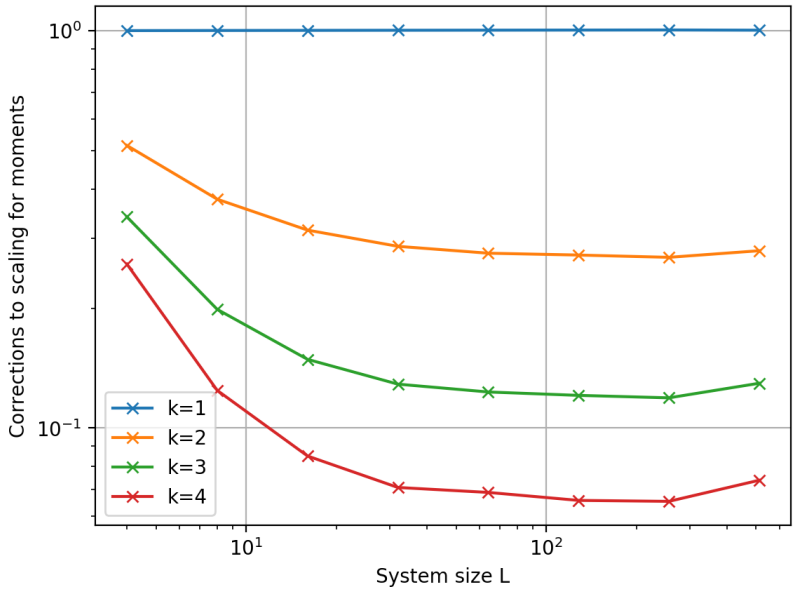

Figure 10: A plot of $\langle s^k \rangle L^{-D(1+k-\tau_s)}$ vs L reveals the corrections to scaling for the avalanche size moments.

5 Conclusion

Through data collapse of rice pile height and avalanche size, this project demonstrated that a boundary-driven 1-dimensional Oslo model displays self-organised criticality. Moment analysis also proved useful in extracting scaling parameters for the avalanche-size probability.

References

[1] Christensen K., and Maloney N., *Complexity and Criticality*, Imperial College Press, London, 2005.

[2] Christensen, K. (2018). *Complexity Project Notes*. Imperial College London, 2019.